Theoretical Modeling and Experimental Verification of Electrochemical Equilibria in the Ba−Ti−C−H_2O System

Sridhar Venigalla[†] and James H. Adair*[,‡]

Department of Materials Science and Engineering, University of Florida, Gainesville, Florida 32611

Received June 12, 1998. Revised Manuscript Received December 8, 1998

The thermodynamic principles controlling the electrochemical synthesis of barium titanate ($BaTiO_3$) films are discussed and explored. a variety of E_h−pH diagrams were generated for the Ba−Ti−C−H_2O system as a function of temperature and whether CO_2 was in the system. Barium titanate is predicted to form at 25 °C and higher temperatures under alkaline conditions. It is demosnstrated that the phase field for $BaTiO_3$ enlarges as a function of pH with increasing temperature in the absence of CO_2. The role of CO_2, although still important in controlling the phase stability of $BaTiO_3$ via the formation of $BaCO_3$, becomes less important under solution pH conditions greater than pH ∼13 and temperatures greater than 100 °C. The theoretical E_h−pH predictions compare favorably with experimentally determined regimes, where $BaTiO_3$ and films in the Ba−Ti−C−H_2O system form through electrochemical reactions.

Introduction

Recent years have witnessed significant advances in the chemical synthesis of advanced ceramic materials for a variety of applications, using techniques such as hydrothermal synthesis, coprecipitation, and sol−gel synthesis. These techniques involve chemical reactions among precursor materials in an aqueous environment. More recently, an electrochemical−hydrothermal technique has been developed to synthesize perovskite type titanate ($BaTiO_3$, $SrTiO_3$, and $CaTiO_3$) thin films on titanium substrates.[1−14] The success of these methods to produce the desired material with specific characteristics depends to a large extent on process parameters, such as pH, composition, electrode potential, and temperature. While several investigators worldwide currently are working on developing and improving methods to synthesize advanced ceramic powders and thin films, very few focused on studying the thermodynamic stability relationships in the relevant systems.[15,16] Such data are crucial to understand the interactions between precursors and other reactants, which ultimately govern the characteristics of the produced material. In addition, understanding electrochemical equilibria in multicomponent systems is critical to evaluate the effect of processing conditions on the electrochemical synthesis of complex oxide thin films.

Electrochemical equilibria in systems containing various elements and their compounds and ionic and neutral species in aqueous environments are represented in the form of E_h−pH diagrams, where E_h is the electric potential for the standard hydrogen electrode.[17−19] These diagrams are extensively used in predicting the stability of materials, usually metals, in aqueous solutions. When interpreted with an understanding of their advantages and limitations, E_h−pH diagrams can provide useful information about the corrosion and passi-

* Corresponding author. E-mail: JAdair@mrl.psu.edu.
[†] Current address: Cabot Performance Materials, County Line Road, Boyertown, PA 19512.
[‡] Current address: 249A MRL, The Pennsylvania State University, University Park, PA 16802.

(1) Yoshimura, M.; Yoo, S.-E.; Hayashi, M.; Ishizawa, N. *Jpn. J. Appl. Phys.* **1989**, *28*, L2007.
(2) Yoo, S.-E.; Hayashi, M.; Ishizawa, N.; Yoshimura, M. *J. Am. Ceram. Soc.* **1990**, *73*, 2561.
(3) Sakabe, Y.; Hamaji, Y.; Hayashi, M.; Ogino, Y.; Ishizawa, N.; Yoshimura, M. *Extended Abstracts*, Fifth U.S.−Japan Seminar on Dielectric and Piezoelectric Ceramics, Kyoto, Japan, 1990; pp 300−303.
(4) Ishizawa, N.; Banno, H.; Hayashi, M.; Yoo, S.-E.; Yoshimura, M. *Jpn. J. Appl. Phys.* **1990**, *29*, 2467.
(5) Kajiyoshi, K.; Ishizawa, N.; Yoshimura, M. *J. Am. Ceram. Soc.* **1991**, *74*, 369.
(6) Kajiyoshi, K.; Yoshimura, M.; Ishizawa, N. *Cer. Trans.* **1992**, *25*, 271.
(7) Bacsa, R.; Ravindranathan, P.; Dougherty, J. P. *J. Mater. Res.* **1992**, *7*, 423.
(8) Pilleux, M. E.; Grahmann, C. R.; Fuenzalida, V. M. *Appl. Surf. Sci.* **1993**, *65/66*, 283.
(9) Dougherty, J. P.; Bacsa, R. *Extended Abstracts*, 6th U.S.−Japan Seminar on Dielectric−Piezoelectric Materials, Maui, HI, 1993; pp 35−38.
(10) Pilleux, M. E.; Fuenzalida, V. M. *J. Appl. Phys.* **1993**, *74*, 4664.
(11) Kajiyoshi, K.; Tomono, K.; Hamaji, Y.; Kasanami, T.; Yoshimura, M. *J. Am. Ceram. Soc.* **1994**, *77*, 2889.
(12) Venigalla, S.; Bendale, P.; Verink, E. D., Jr.; Ambrose, J. R.; Adair, J. H. In *Ferroelectric Thin Films II*, MRS Symposium Proceedings Volume 243, Materials Research Soc.: Pittsburgh, PA, 1992; pp 309−314.
(13) Bendale, P.; Venigalla, S.; Ambrose, J. R.; Verink, E. D., Jr.; Adair, J. H. *J. Am. Ceram. Soc.* **1993**, *76*, 2619.
(14) Venigalla, S.; Bendale, P.; Adair, J. H. *J. Electrochem. Soc.* **1995**, *142*, 2101.
(15) Osseo-Asare, K.; Arriagada, F. J.; Adair, J. H. *Cer. Trans.* **1988**, *1*, 47.
(16) (a)Lencka, M. M.; Riman, R. E. *Chem. Mater.* **1993**, *5*, 61. (b) Lencka, M. M.; Riman, R. E. *Thermochem. Acta* **1995**, *256*, 193. (c) Lencka, M. M.; Anderko, A.; Riman, R. *J. Am. Ceram. Soc.* **1995**, *78*, 2609. (d) Lencka, M. M.; Riman, R. E. *J. Am. Ceram. Soc.* **1993**, *76*, 2649.
(17) Pourbaix, M. *Lectures on Electrochemical Corrosion*; Plenum Press: New York, 1973.
(18) Pourbaix, M. *Atlas of Electrochemical Equilibria in Aqueous Solutions*, 2nd ed.; National Association of Corrosion Engineers: Houston, TX, 1974.
(19) Verink, E. D., Jr. *J. Educ. Modules Mater. Sci. Eng.* **1979**, *1*, 535.

10.1021/cm980424g CCC: $18.00
Published on Web 02/11/1999

vation behavior of metals and solubility data for their compounds and dissolved (ionic and neutral) species, as a function of solution pH and electrode potential. Even though the E_h−pH diagrams are usually constructed for one element−water systems, a few studies in the multielement−water systems have been performed to predict stability relationships in the extraction of metals and beneficiation of ore minerals using hydrometallurgical techniques.[20] Other areas of interest in the application of multielement E_h−pH diagrams include biochemistry and geochemistry.[21] The current work involves development of E_h−pH diagrams to describe electrochemical equilibria in Ba−Ti−C−H_2O system and attempts to verify the theoretical predictions with experimental data published in the literature on the synthesis of $BaTiO_3$ powders and thin films using hydrothermal and electrochemical methods.

Thermodynamic Data

To construct E_h−pH diagrams, the values of the standard Gibbs energies of formation (ΔG_f°) for all the species considered in the system are required. To obtain the most accurate information about the stability of various phases in a system, as many species as possible need to be considered, restricted only by the availability of the thermodynamic data. In addition, it is desirable to obtain the values of ΔG_f° as a function of temperature, to facilitate the construction of the equilibrium diagrams at various temperatures. The standard Gibbs energy of formation for each species can be calculated as a function of temperature, if the values of the heat of formation ($\Delta H°$), and entropy ($S°$) at a reference temperature (usually 25 °C) as well as the heat capacity (C_p°) as a function of temperature (T) are known. From this set of values, the ΔG_f° can be calculated using standard thermodynamic relations:[22]

$$H_T^\circ = \Delta G_{298.15K}^\circ + \int_{298.15K}^{T} C_p^\circ(T)\, dT \qquad (1)$$

$$S_T^\circ = S_{298.15K}^\circ + \int_{298.15K}^{T} \frac{C_p^\circ(T)}{T}\, dT \qquad (2)$$

where H_T° and S_T° are the enthalpy and entropy, respectively, at 1 atm pressure and temperature T. The above equations can also be used to calculate the enthalpy and entropy for the elements. The heat of formation and entropy of formation for compounds are subsequently calculated from the expressions

$$\Delta H_T^\circ = H_T^\circ(\text{compound}) - \sum H_T^\circ\,(\text{elements}) \qquad (3)$$

$$\Delta S_T^\circ = S_T^\circ(\text{compound}) - \sum S_T^\circ\,(\text{elements}) \qquad (4)$$

Finally, the Gibbs free energy for compounds is calculated using the relation

$$\Delta G_T^\circ = \Delta H_T^\circ - T\Delta S_T^\circ \qquad (5)$$

Sources of Thermodynamic Data. Thermodynamic data for several species in the Ba−Ti−C system have been compiled by Lencka and co-workers.[16] For many species, the data are readily available in several existing compilations of thermochemical data.[22−30] For species that are not available in the existing databases, Lenka and Riman[16] have used a computer program[31] that uses the Helgeson−Kirkham−Flowers (HKF) estimation method to predict the standard thermodynamic data. Lenka and Riman have critically evaluated the consistency of these data by verifying the conformity of the relations between the experimental values to the general relations of thermodynamics. The data for additional, usually minor, species that are not considered by Lenka and Riman are obtained from existing thermodynamic databases as well as the database included in HSC Chemistry for Windows,[32] the computer program used to calculate and plot the E_h−pH diagrams in the current work. However, thermodynamic data for some species, particularly Ti^{2+}, Ti^{3+}, and their hydrolyzed species, are not available and therefore are not considered in the calculation of the diagrams.

Reference States. The reference state used in the thermodynamic databases is the most stable form of the pure elements at 298.15 K and 1 atm. The enthalpy and entropy scales of the elements are established as $H°_{element} = 0$ at 298.15 K and 1 atm and $S°_{element} =$ at 0 K and 1 atm.

For aqueous ions, the scales are fixed assuming the enthalpy and entropy values for hydrogen ion (H^+) to be zero in a hypothetical ideal 1 *m* (mol/kg) solution at 298.15 K and 1 atm. Therefore, $\Delta H°(H^+) = 0$ at 298.15 K and 1 atm and $\Delta S°(H^+) = 0$ at 298.15 K and 1 atm. Using these in relation 5, $\Delta G_f^\circ(H^+) = 0$ at 298.15 K and 1 atm.

Estimation at Elevated Temperatures. To obtain the Gibbs energy of formation at elevated temperatures, the standard thermochemical data for each species is converted into the following data set: heat of formation

(20) Ogasawara, T.; da Silva, F. T.; Dutra, A. J. B. *Proceedings of the 47th Annual Congress of the Brazilian Metals Association*; Brazilian Metals Assoc.: Sao Paolo, 1992; pp 267−283.
(21) Garrels, R. M.; Christ, C. L. *Solutions, Minerals, and Equilibria*; Harper and Row Publishers: New York, 1965.
(22) Barner, H. E.; Scheuerman, R. V. *Handbook of Thermochemical Data For Compounds and Aqueous Species*; John Wiley & Sons: New York, 1978.
(23) Barin, I. *Thermochemical Data of Pure Substances*; VCH Publishers: Weinheim, Germany, 1989.
(24) Naumov, G. B.; Ryzhenko, B. N.; Khodakovsky, I. L. *Handbook of Thermodynamic Data*; U. S. Geological Survey: Washington, DC, 1974.
(25) Baes, C. F.; Mesmer, R. E. *The Hydrolysis of Cations*; Wiley-Interscience: New York, 1976.
(26) Barin, I. *Thermochemical Data of Pure Substances*; VCH Verlagsgesellschaft: Weinheim, Germany, 1993.
(27) Knacke, O.; Kubaschewski, O.; Hesselmann, K. *Thermochemical Properties of Inorganic Substances*; Springer-Verlag: Berlin, 1991.
(28) (a) Barin, I.; Knacke, O.; Kubaschewski, O. *Thermodynamic Properties of Inorganic Substances*; Springer-Verlag: New York, 1973. (b) Barin, I.; Knacke, O.; Kubaschewski, O. *Thermodynamic Properties of Inorganic Substances*; Springer-Verlag: New York, Supplement 1977.
(29) Bailey, S. M.; Churney, K. L.; Nuttal, R. L. *J. Phys. Chem. Ref. Data* **1982**, *11*, Suppl. No. 2.
(30) Ruzinov, L. P.; Guljanickij, B. S. *Ravnovesnye Prevrasoenija Metallugiceskin Reaktseij (in Russian)*; Moscow, 1975.
(31) Johnson, J. W.; Oelkers, E. H.; Helgeson, H. C. *SUPCRT92: A Software Package for Calculating the Standard Molal thermodynamic Properties of Minerals, gases, Aqueous Species, and Reactions From 1 to 5000 bar and 0−1000* °C; University of California, Berkeley and Lawrence Livermore National Laboratory, Berkeley, CA, 1991.
(32) Roine, A. *HSC Chemistry for Windows 2.03, Chemical Reaction and Equilibrium Software With Extensive Thermochemical Database*; Outokumpu Research Oy, Pori, Finland, 1994.

Table 1. Free Energy of Formation Data for the Solid Species in Ba−Ti−C−H_2O System at 25, 55, and 100 °C and 1 atm Pressure

oxidation number (Z)			not	ΔG_f°(kJ/mol)		
Ti	Ba	considered[a]	considered	25 °C	55 °C	100 °C
0		Ti		0	0	0
+2		TiO		−513.28	−510.32	−505.90
+2			$Ti(OH)_2$			
+2		TiH2		−105.07	−101.09	−95.00
+3		Ti_2O_3		−1433.82	−1425.07	−1411.97
+3			$Ti(OH)_3$			
+3.33		Ti_3O_5		−2317.29	−2303.03	−2281.72
+3.5		Ti_4O_7		−3213.01	−3193.76	−3164.96
+4		TiO_2(R)		−890.67	−885.10	−876.77
+4		TiO_2(A)		−883.26	−877.69	−869.34
+4			$TiO_2 \cdot H_2O$			
+4			$Ti(OH)_4$			
+6			TiO_3			
	0	Ba		0	0	0
	+1	Ba_2O		−576.98	−573.13	−567.43
	+2	BaH_2		−151.29	−147.37	−141.44
	+2	BaO		−525.34	−522.53	−518.41
	+2	$Ba(OH)_2$		−855.10	−846.44	−833.55
	+2	$Ba(OH)_2 \cdot 8H_2O$		−2779.31	−2723.42	−2637.37
	+2	$BaCO_3$		−1166.06	−1158.15	−1146.33
	+4	BaO_2		−582.27	−577.06	−569.28
+4	+2	$BaTiO_3$		−1572.44	−1563.72	−1550.86
+4	+2	Ba_2TiO_4		−2132.90	−2121.84	−2105.31

[a] TiO_2(R), titanium dioxide, rutile form; TiO_2(A), titanium dioxide, anatase form.

($\Delta H^\circ_{298.15K}$), entropy ($S^\circ_{298.15K}$), and heat capacity (C_p°) given as an empirical function of temperature (T) such that

$$C_p = A + (B \cdot 10^{-3})T + (C \cdot 10^5)T^{-2} + (D \cdot 10^{-6})T^2 \quad (6)$$

where A, B, C, and D are coefficients estimated from experimental data. The heat capacity as a function of temperature is then used in eqs 1 and 2 to generate the heat of formation and entropy as a function of temperature for inclusion in eq 5.

Aqueous Ions. The thermodynamic properties of aqueous ions are traditionally given only at 25 °C, which limits the use of calculations to low temperatures. Therefore, the heat capacity values of these ions are extrapolated to higher temperatures using the entropy correspondence principle developed by Criss and Coble.[33] Using this method, it is possible to extrapolate heat capacity values and estimate them up to 300 °C. According to previous references in the literature,[34−36] extrapolated values have been found to be quite consistent with the experimental data available.

Tables 1 and 2 list the solid and dissolved species, respectively, that are considered and not considered along with the corresponding values of ΔG_f° at 25, 55, and 100 °C. The source of thermochemical data for each species is also cited.

Construction of E_h−pH Diagrams

Types of Reactions Involved. E_h−pH diagrams can represent three types of reactions among the species in the system: reactions involving the transfer of electron(s) only, reactions involving the transfer of H^+ ion(s) only, and the reactions involving both electron and H^+ ion transfer. The reactions involving electron transfer are potential dependent, but independent of pH, and thus are represented as a horizontal line on E_h−pH diagrams. Similarly, reactions involving transfer of H^+ ions will only be dependent on pH and are represented as vertical lines. Reactions involving both electron and H^+ ion transfer are dependent on both pH and potential are and represented as sloped lines in the diagram. The equations for the straight lines representing each type of reaction are calculated from thermodynamic data, as described below.

Reactions Involving the Transfer of Electrons Only. For electrochemical reactions, the familiar Nernst equation can be used to relate the potential and the equilibrium constant for the reaction. Consider the following reaction for the formation of a metal cation:

$$M = M^{n+} + ne^- \quad (7)$$

Note that electrochemical reactions, by convention, are written as oxidation reactions (i.e., electrons are generated by the reaction and appear on the right-hand side of the equation). The equilibrium constant (K) for the above reaction can be written as

$$K = [M^{n+}] \quad (8)$$

By substituting this in the Nernst equation, a linear relationship between the equilibrium potential and the logarithm of the metal cation is obtained

$$E = E^\circ + \frac{2.303RT}{nF} \log [M^{n+}] \quad (9)$$

where E° = the standard electrode potential for the reaction or

$$E^\circ = \frac{\Delta G_r^\circ}{nF} \quad (10)$$

ΔG_r° = the Gibbs free energy change for the reaction or

$$\Delta G_r^\circ = \sum G_f^\circ(\text{products}) - \sum \Delta G_f^\circ(\text{reactants}) \quad (11)$$

R = the universal gas constant, T = the temperature (K), n = the number of electrons transferred, and F = Faraday's constant.

For a given activity of the metal cation, the above relation reduces to a fixed potential value, which is represented as a horizontal line on the E_h−pH diagram, representing the equilibrium between the metal and the cation in solution. The position (E_h value) of this line represents the equilibrium potential attained by the pure metal surface in a solution containing its own ions at that particular activity. This equilibrium can be shifted to a higher or lower potential, either by changing the concentration of the cation in solution or by changing the applied potential. By drawing several lines representing various activities of dissolved species, one can estimate the solubility of the solid substance with reasonable accuracy.

(33) Criss, C. M.; Cobble, J. W. *J. Am. Chem. Soc.* **1964**, *86*, 5385.
(34) Cobble, J. W. *J. Am. Chem. Soc.* **1964**, *86*, 5394.
(35) Mitchell, R. E.; Cobble, J. W. *J. Am. Chem. Soc.* **1964**, *86*, 5401.
(36) Jekel, E. C.; Criss, C. M.; Cobble, J. W. *J. Am. Chem. Soc.* **1964**, *86*, 5404.

Table 2. Free Energy of Formation Data for the Dissolved Species in Ba−Ti−C−H_2O System at 25, 55, and 100°C and 1 atm Pressure.

oxidation number (Z)				DG_f° (kJ/mol)			
Ti	Ba	considered	not considered	25°C	55°C	100°C	ref
+2			Ti^{2+}				
+2			$HTiO_2^-$				
+2			$Ti(OH)^+$				
+2			$Ti(OH)_2$(a)				
+3			Ti^{3+}				
+3			$HTi_2O_4^-$				
+3			$Ti(OH)^{2+}$				
+3			$Ti(OH)_2^+$				
+3			$Ti(OH)_3$(a)				
+4		Ti^{4+}		−354.18	−339.78	−315.54	16
+4		$HTiO_3^-$		−955.88	−959.58	−965.78	16
+4		$TiOH^{3+}$		−614.00	−607.78	−596.49	16
+4		$Ti(OH)_2^{2+}$		−869.56	−867.98	−864.30	16
+4		$Ti(OH)_3^+$		−1092.50	−1094.03	−1095.67	16
+4		$Ti(OH)_4$(a)		−1318.17	−1298.79	−1269.94	16
+4			TiO^{2+}				
+6			TiO_2^{2+}				
+6			$HTiO_4^-$				
+6			TiO_4^{2-}				
	+2	Ba^{2+}		−560.86	−563.12	−566.18	16
	+2	$BaOH^+$		−716.71	−713.40	−708.38	16
	+2	$Ba(CH_3CO_2)_2$(a)		−1299.68	−1278.23	−1244.97	29
	+2	$BaHCO_3^+$		−1153.54	−1147.96	−1138.94	16
	+2	$Ba(HCO_3)_2$(a)		−1734.64	−1715.56	−1686.10	29
	+2	$BaCO_3$(a)		−1103.88	−1094.49	−1079.99	16
		CO_2(a)		−385.99	−383.68	−382.05	16
		HCO_2^-		−351.19	−343.60	−331.84	29
		HCO_2H(a)		−351.19	−343.65	−332.15	29
		CO_3^{2-}		−527.90	−512.57	−487.68	16
		HCO_3^-		−586.85	−576.38	−560.35	16
		H_2CO_3(a)		−623.20	−615.38	−603.22	29
		$C_2O_4^{2-}$		−674.09	−658.60	−634.28	29
		$HC_2O_4^-$		−698.35	−686.39	−668.95	29
		$(COOH)_2$(a)		−674.09	−658.73	−635.15	29
		H^+		0	0	0	

Reactions Involving the Transfer of H^+ Ions Only. In this type of reaction, the Gibbs free energy change of the reaction is related to the equilibrium constant by

$$\Delta G_r^\circ = -RT \ln K = -2.303RT \log K \qquad (12)$$

For the following hydrolysis reaction of a metal ion, the equilibrium constant can be written and substituted in the above equation:

$$M^{n+} + nH_2O \rightarrow M(OH)_n(s) + nH^+ \qquad (13)$$

$$K = \frac{[H^+]^n}{[M^{n+}]} \qquad (14)$$

$$\log K = \frac{-\Delta G_r^\circ}{2.303RT} = -n(\mathrm{pH}) - \log [M^{n+}] \qquad (15)$$

At a given activity of the metal cation, the above equation yields a straight line with a fixed pH value, which is represented as a vertical line on the E_h−pH diagram, indicating the equilibrium between the hydroxide and the metal cation. This line, similar to the horizontal line described above, represents a constant activity for the dissolved metal cation. In other words, it defines a pH value beyond which metal hydroxide can precipitate from a solution containing the metal cations at that particular activity. The position of this line (pH value) can be shifted, by changing the concentration of the dissolved species in relation 15. In the acidic regime, the metal hydroxide can precipitate only at a higher concentration of the cations.

Reactions Involving the Transfer of Both Electrons and H^+ Ions. For electrochemical reactions involving the transfer of both electrons and H^+ ions, the Nernst equation can be used to deduce a straight line relation between the equilibrium potential and pH. For the following equilibrium between a metal and its hydroxide

$$M + nH_2O \rightarrow M(OH)_n(s) + nH^+ + ne^- \qquad (16)$$

$$K = [H^+]^n \qquad (17)$$

$$E = E^\circ = \frac{2.303RT}{nF} = -n(\mathrm{pH}) \qquad (18)$$

the above relation can be represented as a sloped line on the E_h−pH diagram, indicating the equilibrium between the metal and its hydroxide. Along this sloped line, the metal and its hydroxide are in equilibrium, with the same activity of metal cation in solution. Away from this line, only one solid, either the metal or its hydroxide, is stable.

Stability of Water. Each of the E_h−pH diagrams includes a set(s) of sloped parallel lines, a and b, that indicate the thermodynamic stability of water as de-

scribed by the following reactions:[37]

$$H_2(g) \rightarrow 2H^+ + 2e^-$$
$$E_h = 0.000 - 0.0592\ \text{pH, at 25 °C} \quad (19)$$

$$2H_2O \rightarrow O_2(g) + 4H^+ + 4e^-$$
$$E_h = 1.223 - 0.0592\ \text{pH, at 25 °C} \quad (20)$$

In the portion below line a, representing relation 19, if the equilibrium hydrogen pressure is above 1 atm, water under atmospheric pressure is reduced with the evolution of hydrogen. Similarly, in the portion above line b, representing relation 20, if the equilibrium oxygen pressure is above 1 atm, water under atmospheric pressure is oxidized to release oxygen. Between the two lines a and b, the equilibrium pressures of hydrogen and oxygen are both below 1 atm, and the region included between these two lines is the domain of thermodynamic stability for water. Since all aqueous solutions contain water, this domain of stability for water is important, whenever the electrochemical equilibria in aqueous systems are considered. For this reason, all E_h−pH diagrams include the "water" lines a and b. Due to slowness of the kinetics of decomposition of water and high overvoltages of gas production, a significantly wider range of E_h values is actually attainable in the electrochemical studies of aqueous solutions.[21]

Representation of Equilibria. As mentioned in the above section, E_h−pH diagrams contain several lines, each representing a chemical or electrochemical reaction. Depending on the type of reaction, as discussed above, these are represented as horizontal, vertical, and sloped lines. To facilitate easy understanding of the equilibria in E_h−pH diagrams, different line types are used by convention in this paper, to represent each kind of equilibrium. Homogeneous reactions between dissolved (neutral, ionic, and gaseous) species are always represented by thin, dashed lines. These coexistence lines represent the condition wherein the thermodynamic activity of the species on each side of that line is the same. Independent equilibria between dissolved species such as Ba species and Ti species in the Ba−Ti−H_2O system are distinguished by different types of dashed lines. Similarly, independent equilibria between Ba species and C species are distinguished in the Ba−Ti−C−H_2O system. Heterogeneous reactions between dissolved substance(s) and solid substance(s) are represented by thin, solid lines, whereas the equilibria between solid substances are represented by thick, solid lines. The lines representing the effect of temperature for each reaction are individually labeled with a symbol, corresponding to that temperature, as assigned in the legend. Similarly, the lines representing the effect of activity of the dissolved substances on solid−solution equilibria are individually labeled by a digit corresponding to the common logarithm of activity. For example, a line representing 10^{-2} *m* activity is labeled as −2. To preserve the clarity of the diagrams, some of the lines representing the effect of temperature or activity are not labeled, when they can be deduced from other sets of lines that are labeled. Some ionic equilibria exist only at a particular temperature or activity. Such lines are appropriately labeled and care should be taken to note these conditions when interpreting the data. Finally, each line or set of lines is labeled with a number, under which the reaction data is listed in the relevant appendix for each system.

(37) Guenther, W.B. *Chemical Equilibrium: A Practical Introduction for the Physical and Life Sciences*; Plenum Press: New York, 1975; pp 207−228.

Limitations of E_h−pH Diagrams

Similar to any thermochemical analysis, E_h−pH diagrams are inherently subject to several limitations in accurately representing the electrochemical equilibria. As discussed in the following sections, these limitations are important and must be understood before utilizing the diagrams to predict phase stabilities.

Thermodynamic Data. The validity of E_h−pH diagrams depends, to a great extent, on the accuracy of the free energy of formation data for the species considered in the system. Unfortunately, there is no single source that provides the thermochemical data for all the species of interest. As a result, the free energies are obtained from multiple sources, which use a wide variety of techniques to determine or estimate the standard state properties of pure substances. Without a specific procedure to estimate the accuracy of the data, this can lead to a random error in the construction of the E_h−pH diagrams. Even though the free energy data in the current work was obtained from the most recent, critically evaluated sources of thermochemical data, care must be taken while interpreting the stability domains in the diagrams. If the diagram shows that a particular phase is stable relative to the other phase based on a small free energy margin, the unstable phase should only be ignored with reservations.

Species Not Considered. While interpreting the E_h−pH diagrams, one should remember that the diagrams show the equilibria only between the species that are considered in the system. Therefore, the equilibria are valid only if there are no unknown species that are stable in the E_h−pH range of interest and if none of the species that are not considered are stable. In addition, one has to consider all possible reactions among the species in the system, a task made easier with the advent of computers. Considering these difficulties, it is appropriate to say that many of the useful revelations made by the E_h−pH diagrams are negative; for example, one can get an unequivocal answer that two particular phases *cannot* coexist at equilibrium.

Thermodynamics versus Kinetics. As in the case of any thermodynamic calculation, E_h−pH diagrams are constructed with an assumption of thermodynamic equilibrium between the species and indicate regions of thermodynamic stability and boundaries of thermodynamic equilibria. However, these diagrams do not provide any information regarding the kinetics of reactions. Kinetic information, such as reaction rate, activation energy, and reaction pathway are usually obtained by experimental methods.

Activities versus Concentrations. As the E_h−pH diagrams are constructed for activities of the dissolved species, difficulties arise when one attempts to estimate the solubilities of solids or predict their stability as a function of the concentration of the dissolved species.

Activity of a dissolved substance is equal to its concentration in an ideal solution, but all solutions deviate significantly from ideal behavior, except at infinitely dilute concentrations. In a nonideal solution, the activity of an ion differs from its molality by a factor γ, the activity coefficient for that particular ion in a specific solution environment. Activity coefficients can sometimes be estimated fairly accurately, from the knowledge of the ionic strength. However, for complex, multicomponent solutions, activity coefficients need to be predicted on the basis of several solution models.[16] To calculate the solubility of a solid under a given set of E_h−pH conditions, the activities of all contributing dissolved species must be known, along with their activity coefficients. A more direct situation, while utilizing the E_h−pH diagrams, is the prediction of stability of solids at a given composition of the solution. If the stability can be expressed as a function of E_h and pH alone, then no difficulty arises due to lack of activity coefficients, since the equilibrium is independent of dissolved species. But in the case of an equilibrium between a solid and its aqueous species in solution, it is necessary to know the activities of the dissolved species to accurately predict the stability of the solid. Despite this limitation, equilibrium activities obtained from E_h−pH diagrams can be used to estimate the minimum solubility of solids. This can be achieved by the generalization that, when a solid is in equilibrium with a solution, the sum of the activities of all dissolved species containing an element is almost always less than the concentration of that element as determined by chemical analysis. In addition to the above limitations in the use of concentrations as a opposed to activities, E_h−pH diagrams are often drawn at pH values greater than pH 14 to expose phase fields beyond the limits of the accepted pH range. Accordingly, such phase fields should be considered with a degree of reservation.

Discussion of Electrochemical Equilibria

The electrochemical equilibria as revealed by the E_h−pH diagrams constructed for several independent systems among Ba,Ti, and C species are discussed in the following sections. The voluminous reaction data and equilibrium formulas for each reaction in each system are available as Supporting Information.

Ba−H_2O System. Barium, similar to the other alkaline earth metals, is very reactive in aqueous solutions, exerting an extremely low solution potential ($E_h^\circ = -2.908$V at 25 °C), well below the thermodynamic stability domain for water. Ba is unstable with respect to BaH_2, which itself is unstable in the presence of water. Ba and BaH_2 do not coexist, as the coexistence potential lies well above the solution potentials for both Ba and BaH_2. For this reason, E_h−pH diagrams are drawn without considering the formation of BaH_2. The diagram at 25 °C (Figure 1a) is in good agreement with those already reported by Pourbaix.[38] A significant difference, however, is the inclusion of $BaOH^+$ in the current diagrams, in equilibrium with Ba^{2+} under alkaline conditions. Under oxidizing, alkaline conditions, barium peroxide (BaO_2) can be formed, as can be seen in the upper right corner of the E_h−pH diagrams. However, in the thermodynamic stability domain of water, BaO_2 is unstable, converting to barium hydroxide

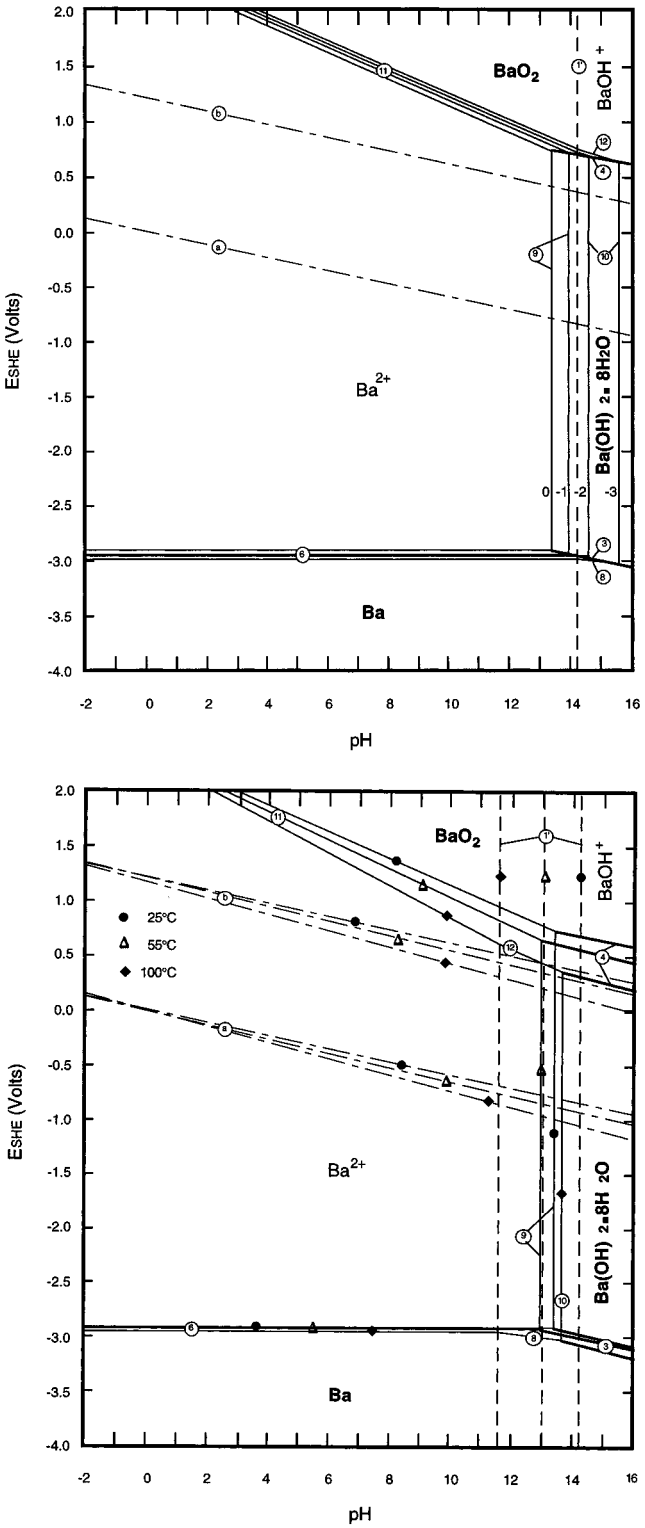

Figure 1. (a) E_h−pH diagram for Ba−H_2O system at 25 °C and 1 atm pressure, not considering the formation of BaH_2. The total activity of dissolved Ba species is varied from 1 to 10^{-3} *m*. (b) E_h−pH diagram for Ba−H_2O system at 25 (●), 55 (△), and 100 °C (◆), and 1 atm pressure, not considering the formation of BaH_2. The total activity of dissolved Ba species is kept constant at 1 *m*. a and b are defined by equations 19 and 20, respectively.

(38) Van Muylder, J.; Pourbaix, M. In *Atlas of Electrochemical Equilibria in Aqueous Solutions*; Pourbaix, M., Ed.; National Association of Corrosion Engineers: Houston, TX, 1974; pp 146−154.

octahydrate, $Ba(OH)_2 \cdot 8H_2O$. Higher temperatures tend to stabilize BaO_2, with the hydration reaction proceeding at lower potentials (Figure 1b). Barium hydroxide octahydrate precipitates at high pH, maintaining an equilibrium with Ba^{2+} (1.0 *m* activity at 25 °C) in solution at pH 13.42. The equilibrium pH is initially lowered with temperature (pH 12.95 at 55 °C), indicating a decreasing solubility of $Ba(OH)_2 \cdot 8H_2O$, as shown in Figure 1b. At 100 °C, however, the presence of $BaOH^+$ in equilibrium with hydroxide extends the solubility of $Ba(OH)_2 \cdot 8H_2O$ to pH 13.7.

Ti−H_2O System. The E_h−pH diagrams for Ti−H_2O are drawn similarly to the Ba−H_2O system, without considering the formation of TiH_2. In addition, these E_h−pH diagrams are drawn with an extended pH range (pH −10 to 15) to fully describe the equilibria between the dissolved species and Ti and its oxides. As seen in Figure 2a, Ti is not stable in the presence of water, but forms a passivating film of oxide on its surface. TiO_2-(R), the rutile phase of titanium dioxide, is the most stable form of native oxide on Ti, in the stability regime of water. TiO_2(R) protects the metal from further deterioration, through most of the pH range, except in the extremely acidic regime,[25] where it dissolves to form $Ti(OH)_2^{2+}$. The other oxides of titanium, TiO and Ti_2O_3, are not stable in the presence of water and convert to TiO_2(R). For this reason, Ti is classified as a base metal, which is easily rendered passive in the presence of water, very similar to aluminum.

The electrochemical equilibria in Ti−H_2O system presented here are in good general agreement with Pourbaix,[39] barring the deviations in the positions of equilibria due to revised thermochemical data. Corrosion and passivation regimes for Ti in the presence of several complexing agents as well as the thermodynamic stability of various forms of the oxides of titanium were well-described by Pourbaix.[39] One notable difference however, is the inclusion of hydrolysis products of Ti^{4+} in the current work. Also, Ti^{2+} and Ti^{3+} ions and their hydrolysis products are not considered in the construction of these diagrams due to the lack of reliable thermochemical data. For this reason, predominance domains for Ti^{2+} and Ti^{3+} do not appear in the current E_h−pH diagrams as they do in Pourbaix's diagrams.[39] However, there is evidence that Ti^{2+} and Ti^{3+} can form by the dissolution of Ti and its oxides in the presence of acidic solutions free from oxidizing agents or by electrolytic reduction of Ti(IV) species.[25] Ti^{2+} and Ti^{3+} are strong reducing agents and their domains of predominance lie well below line a, corresponding to the equilibrium of reduction of water (Figure 2). Ti^{2+} and Ti^{3+} can reduce water, liberating gaseous hydrogen at atmospheric pressure. Accordingly, the exclusion of Ti(II) and Ti(III) species should not affect the accuracy of the diagrams for the most part, as they are readily converted to hydrolyzed Ti(IV) species such as $Ti(OH)_2^{2+}$ between pH 1 and 2 in the stability domain of water.[25] At 25 °C, the only ionic equilibrium that exists in solution is between $Ti(OH)_2^{2+}$ and $Ti(OH)_4$(a), at pH 2.25, as seen in Figure 2a. While the less hydrolyzed

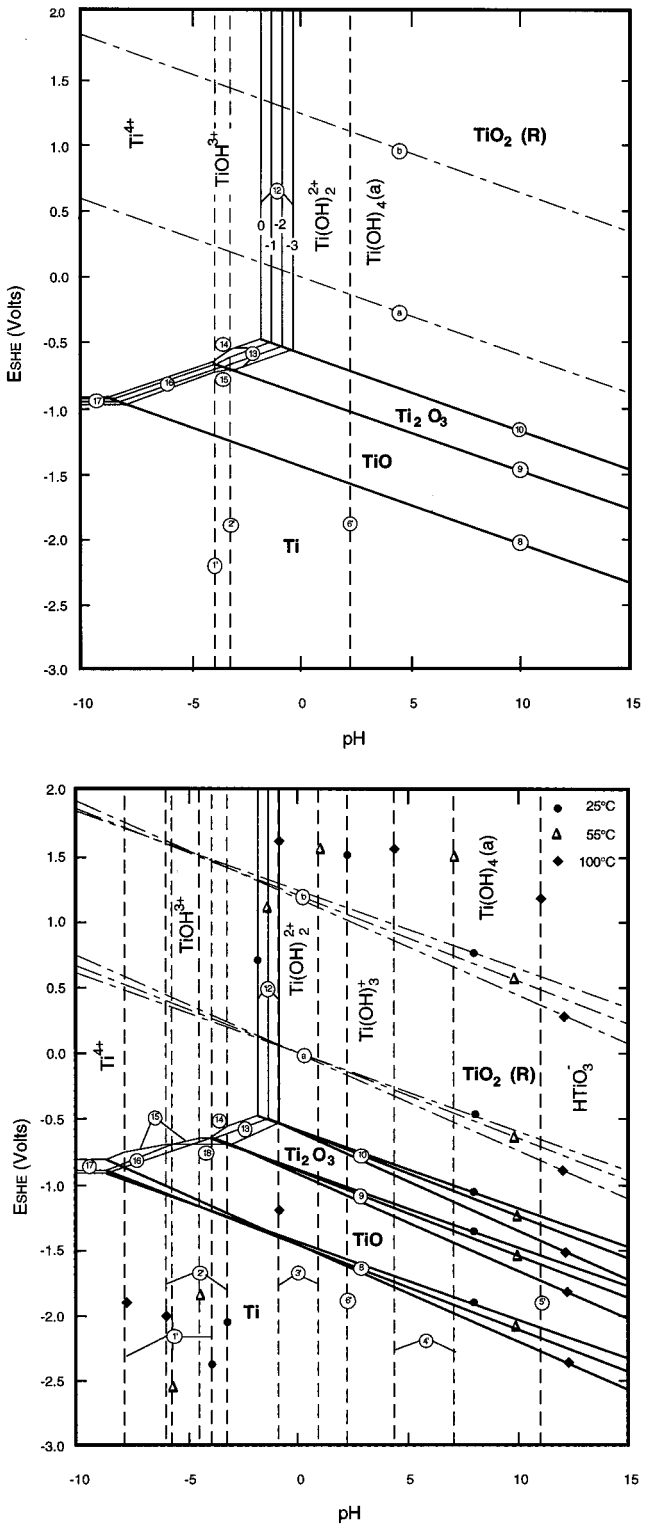

Figure 2. (a) E_h−pH diagram for Ti−H_2O system at 25 °C and 1 atm pressure, for an extended range of pH, not considering the formation of TiH_2. The total activity of dissolved Ti species is varied from 1 to 10^{-3} *m*. (b) E_h−pH diagram for Ti−H_2O system at 25 (●), 55 (△), and 100 °C (◆), and 1 atm pressure, for an extended range of pH, not considering the formation of TiH_2. The total activity of dissolved Ti species is kept constant at 1 *m*. a and b are defined by equations 19 and 20, respectively.

$TiOH^{3+}$ is likely to be stable only at a lower pH, the absence of $Ti(OH)_3^+$ at 25 °C is likely due to the decrease in coordination number when $Ti(OH)_3^+$ is converted to $Ti(OH)_4$(a).[25] These ionic equilibria are consistent with

(39) Schmets, J.; Van Muylder, J.; Pourbaix, M. In *Atlas of Electrochemical Equilibria in Aqueous Solutions*, 2nd ed.; Pourbaix, M., Ed.; National Association of Corrosion Engineers: Houston, TX, 1974; pp 213−222.

the speciation diagram reported for Ti aqueous species.[16] The temperature dependence of the ionic equilibria is illustrated in Figure 2b, showing the presence of $Ti(OH)_3^+$, and $HTiO_3^-$ at higher temperatures. Titanium and its oxides dissolve only with great difficulty, as evident in Figure 2a, where the solid−liquid equilibria can be seen only at extremely low pH. Titanium becomes less and less noble with increasing temperature at high pH, with the stability domain for its oxides extending to lower potentials. However, TiO_2(R) shows higher solubility at elevated temperatures as the equilibrium with $Ti(OH)_2^{2+}$ moves to higher pH values. Formation of metastable TiO_2(A), the anatase form of titanium dioxide, under hydrothermal and electrochemical conditions has been reported.[40,41] Even though it is metastable, crystallization of TiO_2(A) is very dominant at low temperatures, particularly under alkaline conditions (pH >7) and high concentrations of Ti precursors (e.g. $TiCl_4$). Metastable TiO_2(A) converts exothermally to thermodynamically stable TiO_2(R) only at high temperatures (about 1000 °C). It is also found that Ti and TiH_2 do not coexist in equilibrium. This is due to the relatively high temperatures (200−500 °C) and pressures required for the formation of transition metal hydrides.[42]

Ba−Ti−H_2O System. The E_h−pH diagrams for the Ba−Ti−H_2O system are presented in Figure 3. These diagrams primarily represent the phase equilibria between Ti metal and its oxides (not considering the formation of TiH_2), including the complex oxide $BaTiO_3$. The lack of equilibrium between the metal hydrides and pure metal states in aqueous solutions and the overwhelming evidence for the existence of Ba and Ti in their pure, elemental states in equilibrium with their native oxides justify the omission of BaH_2 and TiH_2. Stability domains for BaO_2 and $Ba(OH)_2{\cdot}8H_2O$ are also represented in equilibrium with $BaTiO_3$ and the dissolved species Ba^{2+} and $BaOH^+$. The ionic equilibria between Ti species are distinguished from the equilibrium between Ba^{2+} and $BaOH^+$ by a different type of dashed line, as indicated in the captions. The line(s) corresponding to the equilibrium between Ti metal and TiO intersects the predominance domain for $Ba(OH)_2{\cdot}8H_2O$. The portion of the line(s) present in the $Ba(OH)_2{\cdot}8H_2O$ regime is represented as broken line(s) to clarify that there is no equilibrium between $Ba(OH)_2{\cdot}8H_2O$ and Ti oxides.

It is evident from Figure 3a that $BaTiO_3$ is stable at high pH and moderate potentials. At anodic (positive) potentials higher than ~1.0 V E_h at 25 °C, $BaTiO_3$ tends to decompose to BaO_2 and TiO_2(R), whereas at low potentials (below ~ −1.75 V E_h at 25 °C), $Ba(OH)_2{\cdot}8H_2O$ is the stable phase. At sufficiently high pH, barium titanate is the stable phase in the domain of thermodynamic stability of water, and the only formation reaction is the potential independent conversion of TiO_2(R) in the presence of Ba^{2+} in solution. The concentration of Ba^{2+} determines the equilibrium between

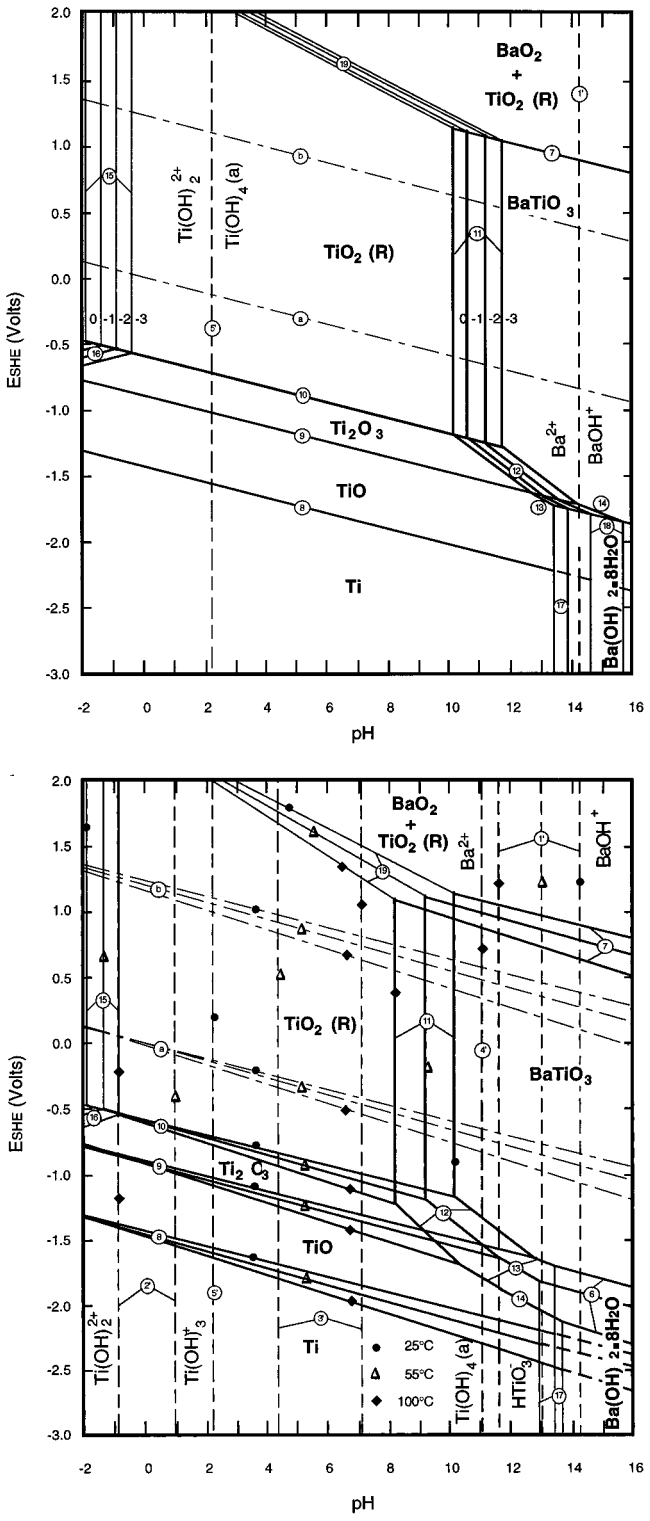

Figure 3. (a) E_h−pH diagram for Ba−Ti−H_2O system at 25 °C and 1 atm pressure. The total activities of dissolved species are independently varied for Ba and Ti, in the range from 1 to 10^{-3} *m*. (b) E_h−pH diagram for Ba−Ti−H_2O system at 25 (●), 55 (△), and 100 °C (◆), and 1 atm pressure. The total activities of dissolved species of Ba and Ti are kept constant at 1 *m* each. a and b are defined by equations 19 and 20, respectively.

TiO_2(R) and $BaTiO_3$. At 1 *m* activity of Ba^{2+}, the minimum pH required to form $BaTiO_3$ at 25 °C is 10.2. At lower concentrations of Ba^{2+}, the equilibrium shifts to higher values of pH, demonstrating the importance of solution alkalinity for synthesizing $BaTiO_3$. The effect

(40) Cheng, H.; Ma, J.; Zhao, Z.; Qi, L. *Chem. Mater.* **1995**, *7*, 663.
(41) Yoo, S.-E.; Yoshimura, M.; Somiya, S. *Proceedings of Materials Research Society International Meeting on Advanced Materials*; Doyama, M., Somiya, S., Chang, R. P. H., Eds.; Materials Research Society: Pittsburgh, PA, 1989; Vol. 3, pp 157−164.
(42) Muetterties, E. L. *Transition Metal Hydrides*; Marcel Dekker: Inc.: New York, 1971; pp 11−32.

of temperature on the stability of $BaTiO_3$ is illustrated in Figure 3b. The equilibrium between $BaTiO_3$ and TiO_2(R) shifts to lower pH at elevated temperatures, extending the stability domain for $BaTiO_3$. However, the stability of BaO_2 extends to lower potentials with increasing temperature, which restricts the predominance of $BaTiO_3$. At higher temperatures, the stability of $BaTiO_3$ is extended at cathodic potentials.

Ba−Ti−C−H_2O System. Addition of carbon to the Ba−Ti−H_2O system drastically affects the electrochemical equilibria, as shown in Figure 4a at various activities of Ba, Ti, and C. The activities of all three elements are the same in each case. The ionic equilibria between C species are distinguished from the ionic equilibria between Ba species by a different type of dashed line. To preserve the clarity of the diagrams, equilibria between Ti species (dissolved and solid) are not shown, as they are not affected by the presence of carbon in the system. Even at an activity as small as 10^{-6} *m*, $BaCO_3$ is stable over a significant range of pH (9−14). Increasing activity extends this domain even further, with $BaCO_3$ being stable over most of the pH range (2−17) calculated at 1 *m* activity. This indicates the importance of eliminating the sources of carbon contamination (e.g., dissolved atmospheric CO_2(g)) while $BaTiO_3$ is synthesized. Ionic equilibria are also affected significantly by the presence of carbon. Barium acetate ion is stable at cathodic potentials, and the ionic equilibria at higher potentials depend on the activities of Ba and C. At low activities (10^{-4} *m* and lower), only Ba^{2+} and $BaOH^+$ are in equilibrium, whereas with increasing activity, other species such as $BaCO_3$(a) at 10^{-2} *m* and $BaHCO_3^+$ at 1 *m* become stable. The effect of temperature on the Ba−Ti−C system at 1 *m* activity is shown in Figure 4b. Temperature dependence of $BaTiO_3$ stability is very similar to that described for the Ba−Ti−H_2O system. The equilibrium between $BaCO_3$ and $BaTiO_3$ shifts gradually to a lower pH with increasing temperature, extending the stability domain for $BaTiO_3$.

Experimental Verification

Using the experimental data published in the literature for hydrothermal and electrochemical synthesis of $BaTiO_3$, the E_h−pH diagrams for Ba−Ti−H_2O and Ba−Ti−C−H_2O have been verified in the following sections. Table 3 lists the experimental conditions along with physical and chemical nature of the reaction products obtained from hydrothermal/electrochemical synthesis of $BaTiO_3$ powders and films as reported in the literature. Since the E_h−pH diagrams indicate thermodynamic *equilibrium* and are drawn for *activities* of dissolved substances, experimental data often is not confined to the predominance domains defined by the E_h−pH diagrams. Moreover, reaction kinetics can be too sluggish for the equilibria to be established. As a result, experimental reactions may involve metastable phases and some of the metastable phases may appear to be stable, equilibrium products. Therefore, while verifying or utilizing the E_h−pH diagrams, one must bear in mind that these diagrams at best show specific "trends" in phase stability, particularly if the equilibria depend on concentrations of dissolved species or involve metastable phases.

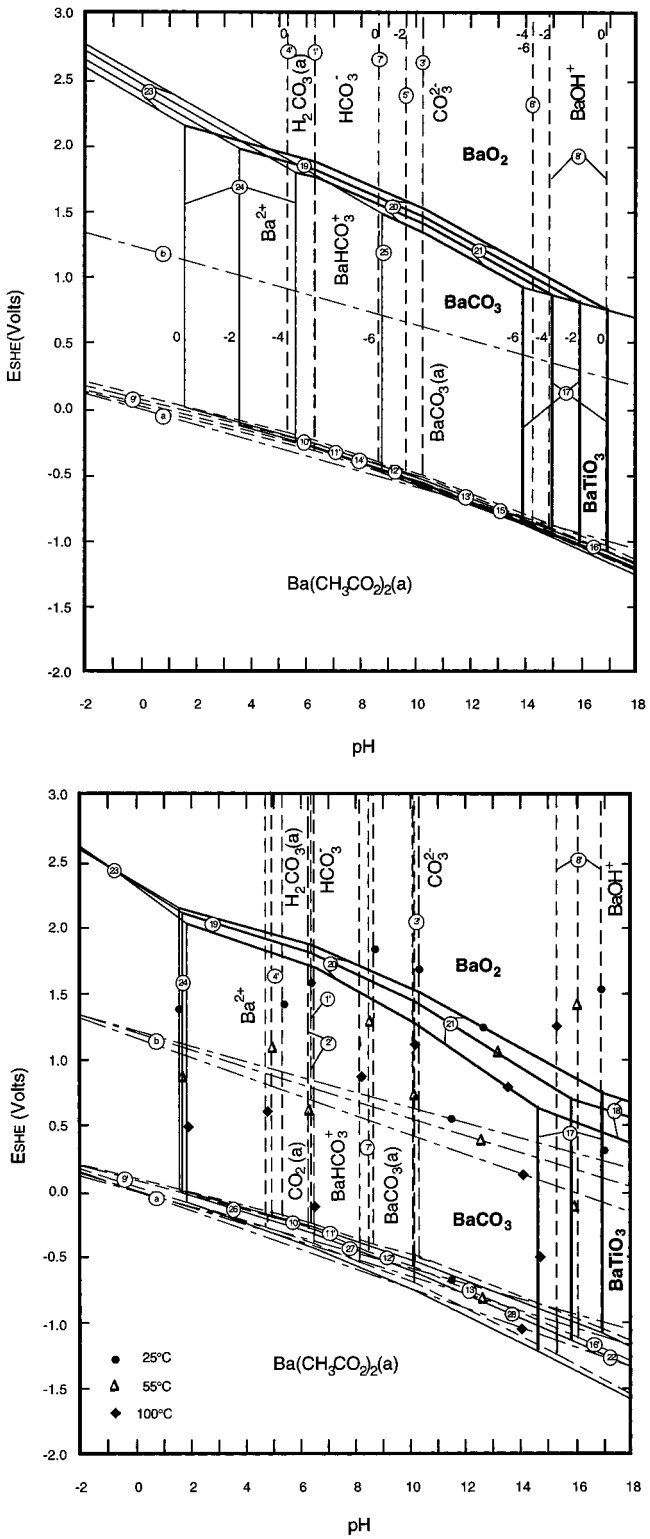

Figure 4. (a) E_h−pH diagram for Ba−Ti−C−H_2O system at 25 °C and 1 atm pressure. The total activities of dissolved species are independently varied for Ba, Ti, and C, in the range from 1 to 10^{-6} *m*. (b) E_h−pH diagram for Ba−Ti−C−H_2O system at 25 (●), 55 (△), and 100 °C (◆), and 1 atm pressure. The total activities of dissolved species of Ba, Ti, and C are kept constant at 1 *m* each. a and b are defined by equations 19 and 20, respectively.

Synthesis of $BaTiO_3$ at Low Temperatures. Hydrothermal and electrochemical syntheses of barium titanate thin films and powders at low temperatures have been reported by several authors. Synthesis tem-

Table 3. Experimental Conditions and Synthesis Products Described in the Published Literature on the Hydrothermal/Electrochemical Synthesis of $BaTiO_3$ Thin Films and Powders[a]

source (ref)	method	form	V (V)	C (mA/cm^2)	T (°C)	pH	electrolyte	products	remarks
41	EC	powder	40−50	50−100	100−250	NM	0.1 N $Ba(NO_3)_2$	$BaTiO_3$ at 250 °C	pure phase
							0.5 N $Ba(NO_3)_2$	$BaTiO_3$ at 200 °C	$BaCO_3$ contamination
							0.1 N $BaCl_2$	TiO_2 (A)	at all temperatures
1	EC	films	NM	10−100	RT−150	NM	0.5 N $Ba(OH)_2$	$BaTiO_3$ at 100−150 °C TiO_2 (A) below 100 °C	
4	HT	films	−	−	120−180	NM	0.5 N $Ba(OH)_2$	$BaTiO_3$ at 180 °C	very thin films (50−100 nm)
							3.0 N $Ba(OH)_2$	$BaTiO_3$ at 150 °C	long reaction times (3−4 h) $BaCO_3$ contamination
5	HT	films	−	−	400−800	NM	0.5−8.0 N $Ba(OH)_2$	$BaTiO_3$ at all temperatures	thicker (0.5−2.5 μm) films, oriented with substrate
								film thickness increased with incresing T, time, and Ba^{2+} concn	no $BaCO_3$ contamination
									well-faceted grain structure
7	EC	films	2−3	10−50	80−200	13	0.4 M $Ba(OH)_2$	$BaTiO_3$, ~2μm thick film at 200 °C, 45 min reaction	thickness increases with time and temp
7	HT	films	−	−	80−200		0.4 M $Ba(OH)_2$	$BaTiO_3$, 600 nm film at 80 °C, 20 h reaction	thin, fine grained films even after long reaction
12,13	EC	Films	2−4	0.5−2.5	55−100	14	0.5M $Ba(CH_3CO_2)_2$	$BaTiO_3$, $BaCO_3$, TiO_2 (amorphous)	lowest synthesis temp reported

[a] HT, hydrothermal; EC, electrochemical; V, cell voltage; C, cell current; T, temperature; TiO_2(A), titanium dioxide, anatase form.

peratures varied from as low as 55 °C[12−14] to about 300 °C.[1,4,41] While the success of synthesizing $BaTiO_3$ at low temperatures verifies the phase stability of $BaTiO_3$, the reason for using higher temperatures and sealed reaction vessels is primarily due to the lack of understanding of the effect of parameters such as pH and solution concentration. Even though TiO_2(R) is the thermodynamically stable precursor phase to $BaTiO_3$, as indicated in the E_h−pH diagrams (Figure 3), an amorphous, metastable, hydrated titanium oxide is more likely to form under highly alkaline conditions, which is widely believed to be the precursor to $BaTiO_3$ in hydrothermal as well as electrochemical processes.[13,43,44] In most cases where a high temperature (above 100 °C) was used to synthesize $BaTiO_3$, the solution pH and/or the Ba^{2+} concentration were significantly lower.[4,41] This "trend" is evident from the temperature dependence of $BaTiO_3$ stability in Figure 3b, where the equilibrium between Ba^{2+} and $BaTiO_3$ gradually shifts to lower pH with increasing temperature. In other cases, a higher temperature was intentionally used to study the process kinetics, microstructure, crystallinity, and morphology.[2,5] Higher synthesis temperatures, in general, improve the kinetics of the electrochemical formation of $BaTiO_3$, yielding thicker films in shorter times. Attempts to electrochemically synthesize $BaTiO_3$ films on Ti substrates at 25 °C were not successful, yielding only an unknown, amorphous phase.[13] However, Klee[45] used the controlled hydrolysis of (Ba,Ti) metal organic precursors to prepare spherical $BaTiO_3$ powders at 30 °C. In the aqueous-based (hydrothermal, electrochemical) processes, reaction of titanium hydrous oxide precursor with Ba^{2+} in solution may be kinetically hindered at temperatures less than 50−60 °C. Hydrolysis of metal organic precursors, on the other hand, leads to a direct precipitation of $BaTiO_3$ from the elemental Ba and Ti precursors, avoiding the kinetically slow conversion of Ti oxide.

Effect of pH and Ba^{2+} Concentration. Concentration of Ba^{2+} ion plays an important role in the synthesis of barium titanate under hydrothermal and electrochemical conditions. Even though the Ba^{2+} concentration is widely varied (0.01−1.5 m) among the reports published in the literature, only Yoshimura and coworkers performed systematic studies on the effect of Ba^{2+} on the stability of $BaTiO_3$ synthesized under electrochemical conditions.[4,41] It has been experimentally confirmed in the above investigations that the minimum temperature required to synthesize $BaTiO_3$ decreases significantly with increasing Ba^{2+} concentration in the electrolyte. Using $Ba(OH)_2{\cdot}8H_2O$ solutions as the electrolyte,[4] $BaTiO_3$ thin films were synthesized on Ti at moderately high concentrations (0.5−1.5 m) of Ba^{2+} in the temperature range of 150−200 °C. At lower concentrations of Ba^{2+} and/or lower synthesis temperatures, only a mixture of $BaTiO_3$ and TiO_{2-x} was obtained, which is in agreement with the phase stability domain for $BaTiO_3$ shown in parts a and b of Figure 3. However, as the electrolyte pH also varies with the concentration of $Ba(OH)_2{\cdot}8H_2O$, the phase stability of $BaTiO_3$ might have been affected by solution pH as well. The effect of Ba^{2+} concentration on the synthesis of $BaTiO_3$ powders by anodic oxidation of Ti in $Ba(NO_3)_2$ solutions[41] confirms the stability of $BaTiO_3$ only above 250 °C with 0.25 m Ba^{2+}. At lower concentrations, either a mixture of $BaTiO_3$ and metastable TiO_2(A) or only TiO_2(A) was obtained. Since the $Ba(NO_3)_2$ solutions possess considerably lower pH values compared to $Ba(OH)_2{\cdot}8H_2O$ solutions, and are relatively insensitive to concentration, these data confirm the effect of Ba^{2+} concentration alone. The effect of solution pH at a constant concentration of Ba^{2+} has also been re-

(43) Prusi, A. R.; Arsov, Lj. D. *Corros. Sci.* **1992**, *33*, 153.
(44) Vivekanandan, R.; Kutty, T. R. N. *Powder. Technol.* **1989**, *57*, 181.
(45) Klee, M. *J. Mater. Sci. Lett.* **1989**, *8*, 985.

ported.[13,14] $BaTiO_3$ thin films were electrochemically synthesized on Ti substrates only above pH 13, in 0.5 *m* $Ba(CH_3CO_2)_2$ electrolytes at 55 °C.

Effect of Applied Potential. As indicated in the E_h−pH diagrams for the Ba−Ti system, the major formation reaction for $BaTiO_3$ is the equilibrium with thermodynamically stable TiO_2(R) and Ba^{2+} ion in solution, which is independent of potential. Even though the actual reaction may involve metastable titanium hydrous oxide precursors as discussed earlier, applied potential has no direct role in the precipitation of $BaTiO_3$. This observation is supported by the data published in the literature on the hydrothermal synthesis of $BaTiO_3$ on Ti substrates.[4,5,7] $BaTiO_3$ could be synthesized without applied potential, even though the rates of deposition were significantly lower (about 4 h for a 100 nm film). Applied potential, however, improves the rate of reaction of the deposition process, probably through the anodic oxidation of Ti, generating the suitable precursor(s) for the precipitation of $BaTiO_3$.[13] In this case, a high anodic potential should have a favorable effect on electrochemical formation of $BaTiO_3$, through the enhanced corrosion of Ti. But the E_h−pH diagrams in Figure 3 indicates the decomposition of $BaTiO_3$ into BaO_2 and TiO_2(R) at even slightly high (>1.0 V E_h) anodic potential. Unfortunately, none of the reports in the literature have done a systematic study on the effect of potential or the current density. Moreover, many studies on the electrochemical synthesis of $BaTiO_3$ were performed galvanostatically, making it difficult to assess the effect of potential. However, a few have reported the cell potentials, which give an insight into the potential dependence of phase stability. At very high cell voltages (40−50 V), only a TiO_2(R) layer was found on the surface of the Ti electrode, while $BaTiO_3$ powder was produced at the bottom of the vessel, through the conversion of fine TiO_2 particles ejected during the breakdown of the anodic TiO_2 film.[41] In another study,[14] use of even a moderate cell voltage (4.0 V) resulted in the formation of $BaCO_3$, probably through the electrolytic breakdown of the barium acetate electrolyte. In an earlier study,[13] depth profile analysis using Auger electron spectroscopy revealed a thicker Ti oxide interface layer between the Ti substrate and the $BaTiO_3$ film grown at higher current density, and the thickness of the film was less than those formed at smaller current densities. From these data, it is apparent that formation of $BaTiO_3$ is not favored at very high potentials, even though the breakdown of $BaTiO_3$ may not proceed at potentials as low as 1.0 V E_h, as indicated in Figure 3.

Effect of Carbon Contamination. Formation of $BaCO_3$ as a contaminant in the synthesis of $BaTiO_3$ is a well-known phenomenon, and appropriate precautions are usually taken to avoid exposure to atmospheric CO_2. However, $BaCO_3$ is always in equilibrium with $BaTiO_3$, even at extremely low concentrations of CO_3^{2-} and Ba^{2+} species, as shown in Figure 4a, and as a result, surfaces of hydrothermally derived $BaTiO_3$ powders or films are always contaminated with $BaCO_3$.[13,16] Although the formation of $BaCO_3$ can be easily avoided during the synthesis step, surface contamination occurs during the postsynthesis washing and handling of $BaTiO_3$.[13] Washing with ammoniated water (at pH 11−12) has been reported as an effective method to minimize surface contamination. This is in agreement with the phase equilibria observed in Figure 4a, where $BaTiO_3$ is stable with respect to $BaCO_3$ at high pH and low activity of dissolved species. The effect of temperature on formation of $BaCO_3$ in the electrochemical synthesis of $BaTiO_3$ was reported.[41] In syntheses at temperatures higher than 250 °C, pure $BaTiO_3$ was formed, whereas a small amount of $BaCO_3$ was always associated with $BaTiO_3$ at synthesis temperatures of 200 °C or less. It is likely that the authors did not remove the dissolved CO_2 from the electrolyte solutions, which might have caused the formation of $BaCO_3$ in the first place. However, these data are consistent with the effect of temperature on the $BaCO_3$/$BaTiO_3$ equilibrium as illustrated in Figure 4b. At a fixed activity of carbon, formation of $BaCO_3$ is less favored at elevated temperatures.

Conclusions

E_h−pH diagrams for Ba−H_2O, Ti−H_2O, Ba−Ti−H_2O, and Ba−Ti−C−H_2O systems are constructed at 25, 55, and 100 °C. Thermochemical data for the solid and dissolved species in the above systems have been acquired from the most recent compilations. The electrochemical equilibria obtained for Ba−Ti−H_2O and Ba−Ti−C−H_2O are consistent with the experimental data published in the literature for the hydrothermal and electrochemical synthesis of $BaTiO_3$.

$BaTiO_3$ is thermodynamically stable at high pH and moderate potentials. Experimental data suggests the feasibility of electrochemically synthesizing $BaTiO_3$ films at potentials higher than indicated by the stability domain for $BaTiO_3$ in the E_h−pH diagrams. This suggests that the decomposition of $BaTiO_3$ is kinetically slower than the formation reaction, so that the equilibrium between BaO_2 and $BaTiO_3$ is not attained. However, at very large anodic potentials, it appears that the formation of $BaTiO_3$ on the anode surface is not favored. The presence of carbon significantly restricts the stability of $BaTiO_3$, even at very low activities, emphasizing the importance of avoiding the exposure to atmospheric CO_2. High synthesis temperatures minimize the $BaCO_3$ contamination by extending the stability domain for $BaTiO_3$ to a lower pH.

Supporting Information Available: Reactions and equilibrium formulas for the various systems discussed. This material is available free of charge via the Internet at http://pubs.acs.org.

CM980424G